Revista de Ciências Agroveterinárias
Universidade do Estado de Santa Catarina (UDESC)

Research Article

Oxidation of Hass Avocado Seed Starch for the Development of Films with Microcrystalline Cellulose

Oxidação do Amido de Semente de Abacate Hass para a Elaboração de Filmes com Celulose Microcristalina

María Elena Yánez-Romero *[1](ORCID 0000-0002-0276-4421), **Luis Alberto Cedeño-Sares** [1](ORCID 0000-0002-4251-358X), **Dayana Macas-Jiménez** [2](ORCID 0000-0003-0846-7556), **Melissa Vidal-Zapata** [3](ORCID 0000-0002-1470-9091), **Hanníbal Lorenzo Brito-Moína** [4](ORCID 0000-0001-7536-857X), **Byron Lapo-Calderón** [1](ORCID 0000-0002-8556-1442), **Carolina Beltrán-Balarezo** [1](ORCID 0000-0003-0806-9240)

[1]Universidad Tecnica de Machala, Machala, Ecuador. *Author for correspondence: myanez@utmachala.edu.ec
[2]Symrise, Machala, Ecuador.
[3]Agua Lajense, Las Lajas, Ecuador.
[4]Escuela Superior Politécnica del Chimborazo, Riobamba, Ecuador.

Submission: August 16st, 2024 | Acceptance: February 1th, 2025

ABSTRACT

This study focused on the development of films based on oxidized starch extracted from Hass avocado seeds with microcrystalline cellulose, as an alternative to conventional plastics to reduce environmental impact. The neat starch was extracted and then subjected to an oxidation process with sodium hypochlorite at different reaction times to improve the physical and functional properties of the films. The reaction time significantly influenced the chemical composition and functional properties of the starch. Starch with a high degree of oxidation (with carbonyl group of 0,029% ± 0,002 and carboxyl group of 0,078% ± 0,003) was selected for film formulation, and an experimental factorial design was conducted to determine the most suitable percentages of D-sorbitol and microcrystalline cellulose to minimize film moisture and solubility and improve water vapor permeability (WVP). It was found that the most suitable percentages of D-sorbitol and microcrystalline cellulose were 1,5% and 0,2% w/v, respectively, to minimize film moisture and solubility; whereas, for WVP they were 1,5% and 0,1% w/v, respectively. However, the results obtained in minimizing film moisture and solubility were very close to those yielded by the percentages 1,5% and 0,2% w/v. In conclusion, this study demonstrated the possibility of using oxidized starch from Hass avocado seeds for film production, with D-sorbitol and microcrystalline cellulose at 1,5% and 0,1% w/v, respectively.

KEYWORDS: Water vapor permeability. Solubility. Moisture. D-sorbitol. Film.

RESUMO

Este estudo focou na elaboração de filmes à base de amido oxidado extraído de sementes de abacate Hass com celulose microcristalina, como alternativa aos plásticos convencionais para reduzir o impacto ambiental. O amido nativo foi extraído e, em seguida, submetido a um processo de oxidação com hipoclorito de sódio em diferentes tempos de reação para melhorar as propriedades físicas e funcionais dos filmes. O tempo de reação influenciou significativamente a composição química e as propriedades funcionais do amido. O amido com alto grau de oxidação (com grupo carbonila de 0,029%±0,002 e grupo carboxila de 0,078%±0,003) foi selecionado para a formulação dos filmes, e foi realizado um delineamento experimental fatorial para determinar as porcentagens mais adequadas de D-sorbitol e celulose microcristalina, visando minimizar a umidade e a solubilidade dos filmes e melhorar sua permeabilidade ao vapor de água (PVA). Constatou-se que as porcentagens mais adequadas de D-sorbitol e celulose microcristalina foram de 1,5% e 0,2% p/v, respectivamente, para minimizar a umidade e a solubilidade dos filmes; enquanto que, para a PVA, foram de 1,5% e 0,1% p/v, respectivamente. No entanto, os resultados obtidos na minimização da umidade e da solubilidade dos filmes foram muito próximos dos obtidos com as porcentagens de 1,5% e 0,2% p/v. Em conclusão, este estudo demonstrou a viabilidade de utilizar amido oxidado de sementes de abacate Hass para a elaboração de filmes, com D-sorbitol e celulose microcristalina a 1,5% e 0,1% p/v, respectivamente.

PALAVRAS-CHAVE: Permeabilidade ao vapor de agua. Solubilidade. Umidade. D-sorbitol. Filme.

INTRODUCTION

In the quest to replace synthetic plastics, research has focused on obtaining new low-cost and biodegradable materials (RIERA & PALMA 2018). However, the production and consumption of synthetic plastics such as polyethylene terephthalate-polyester and polypropylene continue to grow annually worldwide (3.5%), which increases environmental pollution as they take between one hundred and one thousand years to decompose (CALERO et al. 2020, MEDINA et al. 2018, YADAV et al. 2018).

In Ecuador, approximately 14,000 tons of waste are generated daily, 56.2% of which are organic residues such as seeds, fruit, and vegetable peels (MINISTERIO DEL AMBIENTE Y AGUA 2020, RIERA et al. 2018). According to FAOSTAT (2024), avocado production and harvested area have significantly increased, reflecting growing demand. PEDRESCHI et al. (2022) mention that the growing demand for avocados is driving an increase in waste, such as seeds. Seeds of certain fruits represent a non-traditional source of starch that can be used to produce value-added, environmentally friendly bioplastics (BARRAZA & SICHE 2021, CALERO et al. 2020).

The Hass avocado seed is a rich source of starch, with content ranging between 35% and 40% of its total weight, making it an attractive option for starch extraction (CHAPUEL & REYES 2019, CORREA et al. 2019, VIVERO et al. 2019). The amylose and amylopectin that compose the starch of the avocado seed are essential for manufacturing films that act as barriers to oxygen and carbon dioxide and provide better mechanical properties (OSORIO & RUBIANO 2019). However, neat starch has limitations in certain industrial applications due to its low solubility, limited swelling power, higher gelatinization temperature, and high syneresis, making it imperative to modify the starch to reduce retrogradation tendencies, increase solubility, and decrease water permeability (SURI & SINGH 2023). Microcrystalline cellulose (MCC) has been identified as a key additive to improve the mechanical properties of starch-based films, as its integration into starch matrices reinforces the structure of the films, enhancing their strength and stability (LANG et al. 2022).

This research focuses on developing films from oxidized starch derived from Hass avocado seeds, using microcrystalline cellulose as reinforcement to enhance mechanical properties and D-sorbitol to increase flexibility, improve barrier properties, and prevent brittleness. The aim is to reduce the environmental impact of conventional plastics by creating biodegradable alternatives that mitigate pollution and promote the use of renewable resources

This research focuses on the development of films based on oxidized starch from Hass avocado seeds, utilizing microcrystalline cellulose as a reinforcement to improve mechanical properties, and D-sorbitol to enhance barrier properties, flexibility, and prevent brittleness in the films (FONSECA et al. 2018), The goal is to reduce the environmental impact of conventional plastics by creating biodegradable alternatives that mitigate pollution and promote the use of renewable resources.

MATERIAL AND METHODS

Starch extraction from avocado seed

Two hundred fifty grams of mature Hass avocado seeds were collected, washed, and peeled before being cut into small pieces. The pieces were submerged in an antioxidant solution (0.2% w/v sodium metabisulfite) for 24 hours to prevent enzymatic browning. Afterward, the pieces were ground with the same solution, filtered, and decanted to obtain starch granules. The starch granules were then washed with the antioxidant solution and decanted for 24 hours. Upon completion of the time, the washing process was repeated until a clear suspension was obtained, before drying the starch at 48 °C for 24 hours. Finally, the dried starch was sieved using a fine 0.500 µm sieve (SÁNCHEZ et al. 2021).

Oxidation of neat starch

Neat avocado seed starch (ANA) was dissolved in distilled water to obtain a 35% suspension. At a temperature of 35 °C with constant agitation, the pH was adjusted to 9.3-9.34 using 1M NaOH. The starch was then treated with 0.5% v/v sodium hypochlorite (0.7% active chlorine, determined based on the NORMA MEXICANA NMX-K-281-SCFI-2012 2012), for 20 minutes under constant agitation for oxidation, and the pH was adjusted to 9.3 – 9.5 using 1.0M H_2SO_4. The reaction time was evaluated at 30 and 60 minutes, with additional 1M NaOH added if necessary to maintain the pH below 9. The pH was then adjusted to 7.0 using 1.0M H_2SO_4, followed by filtration and washing until a clear filtrate was obtained. The modified starch (AOA) was centrifuged at 2500 rpm for 15 minutes and dried in an oven at 50 °C for 16 hours (ZHOU et al. 2016).

Carbonyl content

To prepare the AOA solution, 2 grams of dry basis starch were mixed with 100 ml of distilled water in a 600 ml beaker. After constantly stirring the solution in a boiling water bath for 20 minutes, it was cooled to 40 °C, and the pH was adjusted to 3.2 with 0.1N HCl. The hydroxylamine reagent was then prepared by diluting 25 g of hydroxylamine hydrochloride in 100 ml of 0.5N NaOH, and 15 ml of this reagent were added to the starch solution, which was maintained in a 40 °C water bath for 4 hours with slow agitation. The excess hydroxylamine in the solution was titrated with 0.1N HCl until a pH of 3.2 was achieved. A blank titration was performed using only the reagent to determine the amount of carbonyl group (%GCn), expressed according to Equation 1 (VANIER et al. 2012, ZHOU et al. 2016).

$$\%GCn = \frac{(V_{ANA} - V_{AOA}) * N * 0.028 * 100}{P} \qquad \text{Eq. (1)}$$

where: V_{AOA} y V_{ANA}, are the volumes in ml of HCl consumed in titrating AOA and ANA, respectively; N, is the normality of HCl; P, is the starch on a dry basis (g).

Carboxyl content

An amount of 0.5-1.0 g of dry basis AOA was weighed and mixed with 25 ml of 0.1N HCl for 30 minutes under continuous agitation. The residue obtained was then filtered, washed, and transferred to a beaker containing 300 ml of distilled water. The mixture was boiled for 8 minutes to achieve gelatinization, and it was titrated with 0.1N NaOH and phenolphthalein. A test was also performed with ANA. The carboxyl content

in the starch (%GCx) was determined using Equation 2 (CHATTOPADHYAY et al. 1997, ZHOU et al. 2016).

$$\%\mathrm{GCx} = \frac{\text{mequi. de acidez}}{100\ \text{g starch}} * 0{,}045 = \frac{(V_{AOA} - V_{ANA}) * N\ * 100}{P} * 0.045 \qquad \text{Eq. (2)}$$

where: V_{AOA} y V_{ANA}, are the volumes in ml NaOH consumed in titrating AOA y ANA, respectively; N, is the normally NaOH; P, is the starch on a dry basis (g).

Chemical composition of the starch

The fiber percentage was measured using the WEENDE method, fat content using the AOAC 2003.06 method, moisture content using the AOAC 925.10 method, protein content using the DHUMAS method, and pH using INEN 526. The carbohydrate content was calculated by the difference, which involves subtracting the percentages of fiber, fat, moisture, protein and ash from 100 (%Carbohydrates = 100 – % fiber - % fat - % moisture - % protein - % ash.

Fourier Transform Infrared Spectroscopy

The FTIR spectra of ANA and AOA were recorded using a Fourier Transform Infrared Spectrometer (Jasco FTIR-4000) with a resolution of 0.9 cm^{-1} and a wavelength range of 500 to 4000 cm^{-1}. For the preparation of starch granules, a small amount of each sample was extracted and compressed into pellets with a KBr cell, which were then placed in the FTIR reading lens. The absorption spectrum was acquired using the Fourier Transform Infrared Radiation Absorption technique, generating a spectroscopic graph of the specific absorption bands of the chemical bonds present in the samples. The starch samples were cleaned, dried, and packed at a temperature of 20 ± 0.7 °C and a relative humidity of 5 ± 1.4% to avoid any influence on the measurements.

Functional properties of starch

Centrifuge tubes were used to mix 1.25 g of dry basis avocado seed starch with 30 mL of distilled water heated to 60 °C. The mixture was stirred and subjected to a water bath for 30 minutes at 60 °C, with agitation every 10 minutes. It was then centrifuged at 4900 RPM for 30 minutes at room temperature. The supernatant was separated, and its volume was measured by taking a 10 mL sample and placing it in an oven at 70 °C for 16 hours in Petri dishes. The tubes with the gel and the dishes with the solids were weighed after each treatment. The functional properties—swelling power (SP), water absorption index (WAI), and water solubility index (WSI)—were determined using Equations 3, 4, and 5, respectively (MURILLO-MARTÍNEZ et al. 2021).

$$\mathrm{SP} = \frac{Weight\ of\ gel\ (g)}{Sample\ weight(g) - Soluble\ weigth\ (g)} \qquad \text{Eq. (3)}$$

$$\mathrm{WAI} = \frac{Weigth\ of\ gel\ (g)}{Sample\ weigth\ (g)} \qquad \text{Eq. (4)}$$

$$\mathrm{WSI} = \frac{Soluble\ weight\ (g) * Volume\ of\ supernatant\ (mL) * 10}{Sample\ weight\ (g)} \qquad \text{Eq. (5)}$$

Preparation of oxidized starch films

To prepare AOA films with microcrystalline cellulose (MCC), the starch with the highest degree of oxidation (carboxyl groups, 0.078%, and carbonyl groups, 0.029%),

corresponding to the 60-minute reaction time, was used. Microcrystalline cellulose (MCC) is an additive that enhances the mechanical properties of starch-based films by reinforcing their structure, thus improving their strength and stability (LANG et al. 2022). MCC solutions were prepared at different concentrations (0.1% w/v and 0.2% w/v) and mixed with a 4% w/v starch solution, bringing the mixture to the gelatinization temperature with a waiting time of 20-30 minutes. The plasticizer D-sorbitol was then added at different concentrations (0.5% w/v, 1.5% w/v), along with 3% w/v commercial vinegar (5% acidity). The solution was left to rest until it reached 40 °C and was then poured into non-stick molds before being placed in an oven for 16 hours at 50 °C. (OTHMAN et al. 2019, RUILOBA et al. 2018).

Characterization of oxidized starch films

The moisture content of AOA films with MCC was determined using a thermobalance at 180 °C, with 1 gram of sample for each measurement.

The solubility of the films was calculated as the percentage of dry matter solubilized after immersion in distilled water at 25 °C for 24 hours. The films were cut into 2x2 cm squares, weighed, and immersed in 50 ml of distilled water at room temperature. After 24 hours, they were filtered and dried in an oven at 105 °C for 24 hours, and their final weight was recorded. Equation 6 was used with the initial and final weights obtained (FONSECA et al. 2018).

$$\%\, Solubility\ = \frac{\text{initial dry mass (g)} - \text{final dry mass (g)}}{\text{initial dry mass (g)}} \times 100 \qquad \text{Eq. (6)}$$

Water vapor permeability (WVP) was determined using the water method. The films were fixed in permeability cells with distilled water (100% RH) and placed in a desiccator with a thermohygrometer. The weight of the cup was recorded every hour for 6 measurements. The water vapor transmission rate (WVTR) was calculated from the slope obtained from the regres sion analysis of the cup weight loss results as a function of time, divided by the film area (SANTOS et al. 2017). The WVP was calculated using Equation 7 described by GÓMEZ & JIMÉNEZ (2022).

$$WVP = \frac{(WVTR * I)}{\Delta P} = \frac{(WVTR * I)}{\left(\frac{\Delta HR * PVAPSAT}{100}\right)} \qquad \text{Eq. (7)}$$

Where: ΔHR, relative humidity gradient between the environment and the cell; PVAP SAT saturated pure water vapor pressure (at 25 °C, it is 3.160 kPa); I, thickness of the film (mm).

Stadistical Analysis

This section explains the statistical procedures used to analyze the data obtained. A 2^2 factorial design was applied, and a one-way analysis of variance (ANOVA) was performed to determine if there were significant differences among the groups. To discriminate between the means, Fisher's Least Significant Difference (LSD) method was used. This procedure allowed for identifying which means were significantly different from each other by assigning different letters to those with statistically significant differences.

RESULTS AND DISCUSSIONS

Starch extraction yield from avocado seed.

The yield obtained for ANA extraction with metabisulfite, 36.2% ±0.013, is considerably higher than those reported by MACENA et al. (2020) and MARTINS et al. (2022), whose yields were 10.67% and 19.54%, respectively. RUILOBA et al (2018) and MARTINS et al. (2022) have indicated that various factors can influence starch extraction yield, such as the extraction method, the variety of the fruit, and its degree of ripeness.

Degree of oxidation through carbonyl and carboxyl groups

Table 1 shows the effect of reaction time (30 and 60 min) on the carbonyl groups (%GCn) and carboxyl groups (%GCx) of the starches. An analysis of variance was conducted, and the results indicate a significant effect of reaction time on the degree of oxidation.

Table 1. Content of carbonyl and carboxyl groups in neat and oxidized starch at two reaction times.

Starch	TR*	%GCn (CO/100GU)	%GCx (COOH/100GU)
ANA	0 min	0.000±0.000^{a}	0.000±0.000^{a}
AOA30	30 min	0.085±0.007^{b}	0.036±0.001^{b}
AOA60	60 min	0.029±0.002^{c}	0.078±0.003^{c}

* TR: Reaction time. ANA: Neat avocado seed starch; AOA30: Starch oxidized at a TR of 30 min; AOA60: Starch oxidized at a TR of 60 min. Arithmetic mean of three repetitions ± standard error; means within a column with different letters are significantly different (p≤0.05).

AOA30 shows a significant increase in carbonyl groups, while AOA60 decreases. This result aligns with the research of ZHOU et al. (2016) and CARHUALLAY et al. (2020), which suggest that OH- groups, precursors of carbonyl groups, oxidize into carboxyls at a much faster rate, reducing the number of carbonyl groups as oxidation time increases.

The amount of carboxyl groups in AOA60 is much higher than in AOA30, suggesting that carboxyl groups become the primary product as oxidation progresses. This result is consistent with the findings of MARGARETTY et al. (2019), which indicate that longer reaction times and increased interaction between the oxidizing agent and starch molecules lead to an increase in carboxyl groups. Additionally, the linear distribution of amylose produces more carboxyl groups in the polymer chain, which prevents retrogradation and degradation of amylose.

Factors such as the concentration of active chlorine in the oxidizing agent, the nature of the raw material, pH, temperature, and the oxidation time used, according TO BUSTILLOS-RODRÍGUEZ et al. (2019), SUKHIJA et al. (2017), and FONSECA et al. (2015), influence the increase in the degree of oxidation.

Chemical composition of neat and oxidized starch.

The chemical composition of ANA and AOA at two reaction times is shown in Table 2. Except for protein and moisture ($p<0.05$), all parameters comply with the Shapiro-Wilk statistic ($p>0.05$). AOA30 and AOA60 showed increases in carbohydrates, protein, fiber, and pH, while fat content decreased. AOA30 had lower moisture content, while AOA60 had higher moisture content. These results are consistent with other studies demonstrating that starch oxidation can alter its chemical

composition. Moreover, the variety and type of oxidizing agent used influence the properties of oxidized starches (BUSTILLOS-RODRÍGUEZ et al. 2019).

The moisture values of ANA were similar to those reported by JIMÉNEZ et al. (2022a), while the moisture, protein, and fat values differed from those obtained by MACENA et al. (2020), although similarities in protein content were found with BARBOSA et al. (2016). The variability in the results could be due to different agroclimatic conditions, varieties, and drying conditions of the avocado seeds (MARTINS et al. 2022).

Table 2. Chemical composition of neat and oxidized starch at two reaction times.

Starch	%Carbohydrate	%Protein	%Fat	%Fiber	%Moisture	pH
ANA	41.213±0.531[a]	4.540±0,180[a]	0.563±0.030[a]	0.030±0.001[a]	12.843±0.133[a]	4.883±0.090[a]
AOA30	42.813±0.211[b]	4.606±0,455[a]	0.340±0.017[b]	0.046±0.005[b]	10.910±0.085[b]	5.620±0.017[b]
AOA60	45.206±0.847[c]	9.990±0,288[b]	0.426±0.015[c]	0.083±0.005[c]	13.270±0.026[c]	6.126±0.005[c]

ANA: Neat avocado seed starch; AOA30: Oxidized starch, reaction time 30 min; AOA60: Oxidized starch, reaction time 60 min. Arithmetic mean of three repetitions ± standard error; means within a column with different letters are significantly different ($p \leq 0.05$).

The decrease in fat content in AOA30 and AOA60 may be attributed to the oxidative attack on the unsaturated fatty acids present in the starch during the oxidation process (SCHAICH 2016). The pH of the AOA samples is similar to those reported by MACENA et al. (2020), who suggest that the reagents used in the modification procedure may have influenced the pH variations of the starches, as the alkaline pathway increases pH.A decrease in moisture content was observed in AOA30.

RUILOBA et al. (2018) suggest that this could be related to environmental factors, storage methods, or the maturity of the avocado. However, in AOA60, an increase in moisture was recorded, which may be due to the presence of carboxyl and carbonyl groups in the modified starch, as explained by RINCÓN et al. (2007). These groups disrupt the linearity of amylose and the linear sections of amylopectin, decreasing intermolecular clustering and promoting granule hydration due to the affinity of carboxyl groups. Additionally, AYO OMOGIE et al. (2022) suggest that the degradation of cell walls during the oxidation process is likely responsible for the increase in crude fiber in the AOA samples.

Fourier Transform Infrared Spectroscopy of the starches

Starch, composed of amylose and amylopectin, shows two characteristic regions in spectroscopy: the O-H and C-H stretching vibrations (between 3650-3000 cm^{-1}) and the carbohydrate fingerprint region (between 1200-800 cm^{-1}) (DAO et al. 2017, JIMÉNEZ et al. 2022b).

In Figure 1(A-C), peaks can be identified from 3500 to 500 cm^{-1}. The peaks around 3290-3296 cm^{-1} can be attributed to O-H stretching in starch, slightly altered by oxidation, reflecting changes in its hydrated structure; and the peaks between 995-929 cm^{-1} correspond to =C-H bending, while the formation of peaks at 860 cm^{-1} in oxidized samples indicates the incorporation of carbonyl and carboxyl groups (FASUAN et al. 2018).

The C-H bond stretches are found between 2909-2940 cm^{-1}, and the peaks at 1639.89 cm^{-1}, 1640.52 cm^{-1}, and 1640.17 cm^{-1} are associated with water absorption in the starch structure. Additionally, the peaks at 1149 cm^{-1} and near 1076 cm^{-1} could be linked to C-O stretching in the glycosidic units (ARAÚJO et al. 2020, WIJAYA et al. 2019).

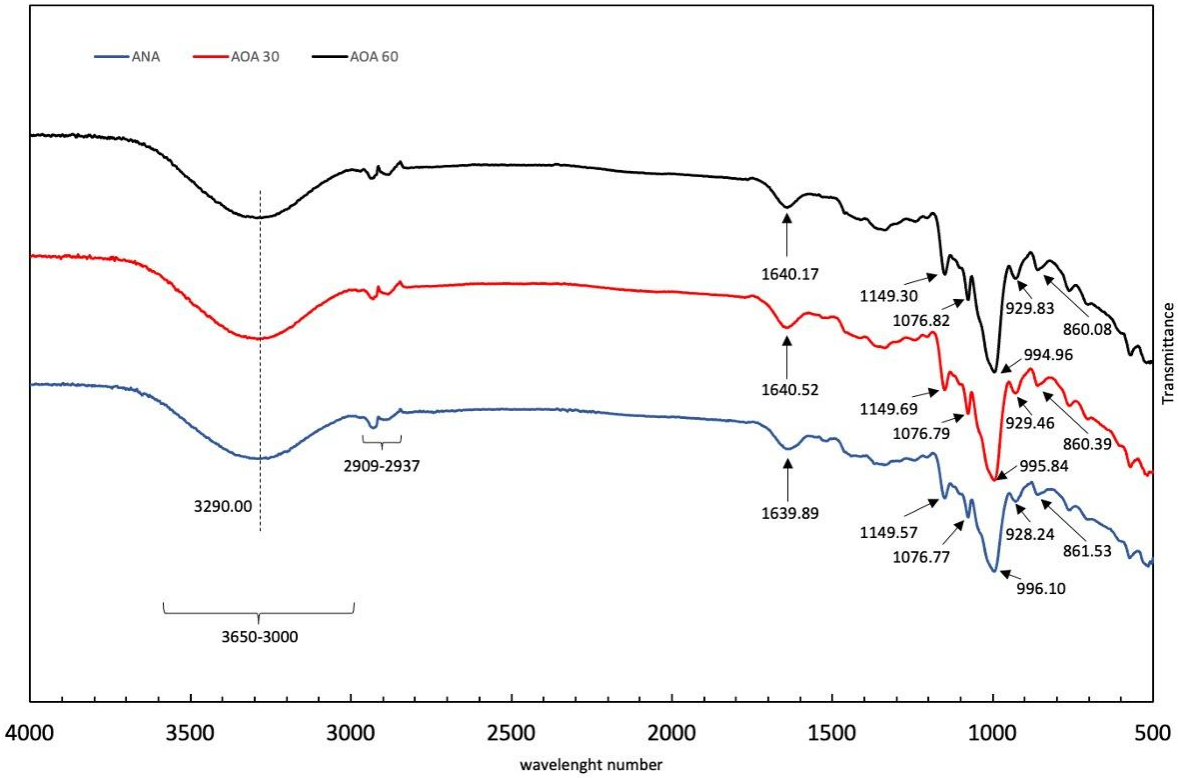

Figure 1. FTIR spectra for neat and oxidized starches: A) Neat avocado seed starch, ANA; B) Starch oxidized at 30 min., AOA30; C) Starch oxidized at 60 min., AOA60.

Functional properties of neat and oxidized starch.

Table 3 presents a comparison of the functional properties of neat starch and oxidized starch, showing how these properties vary depending on the reaction time. Neat starch has higher %SP and %WAI values compared to the oxidized starches AOA30 and AOA60, but its %WSI is lower. On the other hand, AOA60 shows the highest %WSI values but has the lowest %SP and %WAI values. This suggests that as the reaction time increases, %SP and %WAI decrease while %WSI increases.

Table 3. Functional properties of neat and oxidized starch at two reaction times.

Starch	TR*	%PH	%IAA	%ISA
ANA	0 min	2.031±0.014^{a}	2.022±0.014^{a}	0.418±0.007^{a}
AOA30	30 min	1.991±0.007^{b}	1.982±0.007^{b}	0.470±0.006^{b}
AOA60	60 min	1.957±0.009^{c}	1.957±0.009^{c}	0.559±0.026^{c}

* TR: Reaction time; %SP: Swelling power; %WAI: Water absorption index; %WSI: Water solubility index. Arithmetic mean of three repetitions ± standard error; means within a column with different letters are significantly different ($p \leq 0.05$).

The %SP and %WAI values of ANA are lower than those reported by SÁNCHEZ et al. (2021), but the %WSI is higher. According to SOLARTE-MONTÚFAR et al.

(2019), the amount of %SP, %WAI, and %WSI in starches is likely due to the high content of phosphate groups in amylopectin, which generate repulsion in adjacent chains, increasing hydration by weakening the bonds within the crystalline part of the granule.

The modification of starch increased %ISA and decreased %PH and %IAA, as observed in the studies by SOLARTE-MONTÚFAR et al. (2019) and VANIER et al. (2012). According to SÁNCHEZ et al. (2021), the %PH of starch depends on its amylopectin content and water absorption capacity, while %IAA measures the amount of amylose released during granule disintegration. CARHUALLAY et al. (2020) link the decrease in %IAA in oxidized starch with increased oxidation time or hypochlorite concentration used, reducing water retention capacity. VANIER et al. (2012) state that oxidized starch has lower %PH and higher %ISA due to depolymerization of amylose and amylopectin chains, with amylose being most affected. Amylopectin is responsible for the swelling and pasting of starch granules, though it can be inhibited by amylose and lipids

The modification of starch increased %ISA and decreased %PH and %IAA, as observed in the studies by SOLARTE-MONTÚFAR et al. (2019) and VANIER et al. (2012). According to SÁNCHEZ et al (2021), the %PH of starch depends on its amylopectin content and water absorption capacity, while %IAA measures the amount of amylose released during granule disintegration. CARHUALLAY et al. (2020) link the decrease in %IAA in oxidized starch with increased oxidation time or hypochlorite concentration used, reducing water retention capacity. VANIER et al. (2012) state that oxidized starch has lower %PH and higher %ISA due to depolymerization of amylose and amylopectin chains, with amylose being most affected. Amylopectin is responsible for the swelling and pasting of starch granules, though it can be inhibited by amylose and lipids.

Statistical analysis of the physical and barrier properties of oxidized starch-based films.

Table 4 shows the results for %Moisture, %Solubility, and %WVP at different percentages of %D-sorbitol and %MCC for each treatment. These results were evaluated using the statistical program Statgraphics Centurion XVI.

Table 4. Results of %Moisture, %Solubility, and %WVP of the oxidized starch-based film.

Treat.	%D-Sorbitol	%MCC	%Moisture	%Solubility	% WVP (g mm/m2 h kPa)
1	0.5	0.1	2.372±0.035 ^{d}	27.876±1.228^{d}	2.78E-04±9.504E-06^{d}
2	0.5	0.2	2.320±0.014^{bc}	24.921±0.972^{c}	2.20E-04±3.718E-05^{c}
3	1.5	0.1	2.375±0.028 ^{d}	22.194±0.533^{b}	1.81E-04±2.143E-05^{a}
4	1.5	0.2	2.270±0.001 ^{a}	20.577±0.476^{a}	2.94E-04±2.877E-05^{b}
5	0.5	0.1	2.360±0.014^{cd}	26.831±0.184^{d}	2.48E-04±3.943E-05^{d}
6	1.5	0.2	2.275±0.014^{ab}	21.313±1.212^{a}	2.38E-04±2.719E-05^{b}
7	1.5	0.1	2.360±0.014^{cd}	21.090±0.569^{b}	1.60E-04±8.494E-05^{a}
8	0.5	0.2	2.310±0.014^{ab}	24.681±0.731^{c}	1.88E-04±1.905E-05^{c}

%Oxidized avocado seed starch = 4; %Vinegar = 3Treat.: Treatment with its replica; WVP: Water vapor permeability; MCC: Microcrystalline cellulose. Arithmetic mean of three repetitions ± standard error; means within a column with different letters are significantly different (p≤0.05).

According to the analysis of variance (Table 5), it is observed that both factor A (%D-sorbitol) and factor B (%MCC) have a significant effect ($p<0.05$) on the moisture and solubility percentage of the polymer matrix in the films. However, the interaction between both factors (AB) does not show a significant effect ($p>0.05$) on the solubility. Regarding water vapor permeability, it is evident that the interaction between both factors (AB) has a significant effect ($p<0.05$), while factor A and factor B do not show a significant difference ($p>0.05$).

Table 5. Analysis of variance for the physical and barrier properties of oxidized starch-based films.

Source	% Moisture	% Solubility	% WVP
A: %D-Sorbitol	0.0138	0.0016	0.1341
B: %MCC	0.0005	0.0326	0.0924
AB	0.0191	0.1203	0.0019

WVP: Water vapor permeability; MCC: Microcrystalline cellulose. Arithmetic mean of three repetitions, significant effect $p<0.05$.

Figure 2A shows that both D-sorbitol, MCC and the interaction between them (AB) in the film formulations significantly decrease the moisture content. D-sorbitol reduces moisture due to its strong hydrogen bonds and its ability to form resistant intermolecular bonds with the polymer matrix. Meanwhile, MCC exhibits a high capacity for water absorption and retention due to its crystalline structure and the close proximity between its molecules. Both components limit the interaction of water molecules with the film and reduce the amount of retained water. These results are consistent with the findings of FAUST et al. (2022), HAZROL et al. (2021), HIDAYATI et al. (2015) y MILLER et al. (2021).

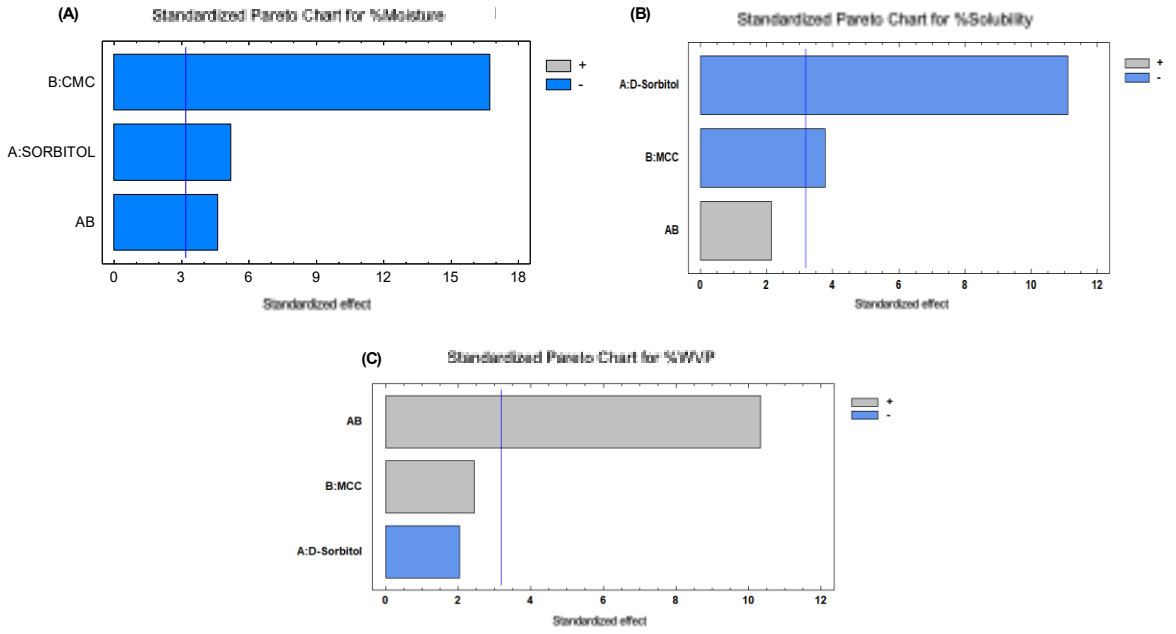

Figure 2. Influence of D-Sorbitol, MCC, and AB on the increase or decrease of %Moisture (A), %Solubility (B), and %WVP (C) in the films. Keys: AB: Interaction between D-Sorbitol and MCC; WVP: Water vapor permeability; MCC: Microcrystalline cellulose.

The solubility of the films is significantly influenced by D-sorbitol and MCC (Figure 2B). The nature and concentration of the plasticizer are key factors in this property, as many are hydrophilic and reduce the interaction between starch molecules, allowing water ingress (MERCI et al. 2019). On the other hand, MCC decreases solubility by interacting with the more soluble regions of the starch. Although the interaction between both factors (AB) increased solubility, this increase was not significant. This increase can be attributed to carboxyl groups in the polymer chain and repulsive forces that produce greater water mobility, as reported in previous studies (EL HALAL et al. 2015).

Finally, Figure 2C shows that the combination of AB (% D-sorbitol and % MCC) in the film significantly increases WVP; while D-sorbitol and % MCC, on their own, do not have a significant effect on WVP. However, the effects of the AB combination may vary depending on the amount of plasticizer present in the film and the interaction between the components. According to BALLESTEROS-MÁRTINEZ et al. (2020), D-sorbitol, although less hydrophilic, can modify the three-dimensional distribution of the matrix in the film at high concentrations, reducing molecular cohesion and increasing water absorption around the hydrophilic regions of the film, which increases WVP. On the other hand, the research by MERCI et al. (2019) and YAO DÉSIRÉ et al. (2021) indicates that a greater presence of MCC can decrease WVP by preventing water vapor from spreading through the film.

Adjusted regression models for the physical and barrier properties of oxidized starch-based films

The adjusted regression models for oxidized starch films demonstrated high significance (R^2 and adjusted R^2 by degrees of freedom >95%) of the predictor variables D-Sorbitol and MCC in predicting %Moisture, %Solubility, and %WVP (Table 6). The relationship between these variables and the corresponding response variable is shown in each model equation, providing valuable information for assessing the quality and predictive capability of the models. The models have the potential to improve the formulation and performance of oxidized starch films in specific applications, and the encouraging results suggest great potential for their development and application.

Table 6. Adjusted regression models for the physical and barrier properties of oxidized starch-based films.

Response variable	Adjusted model equation	R^2 (%)	AjustedR^2 by g.l. (%)
%Moisture	%Moisture = 2.40125 – 0.0375*D-Sorbitol – 0.325*MCC – 0.4*D-Sorbitol*MCC	99.1036	98.4313
%Solubility	%Solubility = 33.6895 – 7.567*D-Sorbitol – 34.8025*MCC + 18.555*D-Sorbitol*MCC	97.9465	95.2084
%WVP	%WVP = 0.0004455 – 0.000247*D-Sorbitol – 0.0013625*MCC + 0.001545*D-Sorbitol*MCC	97.8796	95.0525

Response Surface analysis

The relationship between the evaluated factors (D-sorbitol and MCC) and their impact on the moisture content, solubility, and WVP of oxidized starch-based films is visualized in Figure 3 (A-C). The most suitable values to minimize %Moisture and %Solubility in the colloidal matrix were 1.5% D-Sorbitol and 0.2% MCC, while to minimize %WVP, the values were 1.5% D-Sorbitol and 0.1% MCC. Increasing the percentages of D-sorbitol and microcrystalline cellulose decreases moisture content and solubility but increases WVP within the study range. Therefore, the values of 1.5% D-Sorbitol and 0.1% MCC can be selected as the most suitable, as the %Moisture and %Solubility percentages obtained with 1.5% D-Sorbitol and 0.2% MCC are close. These results are relevant for the formulation of oxidized starch-based films in specific applications.

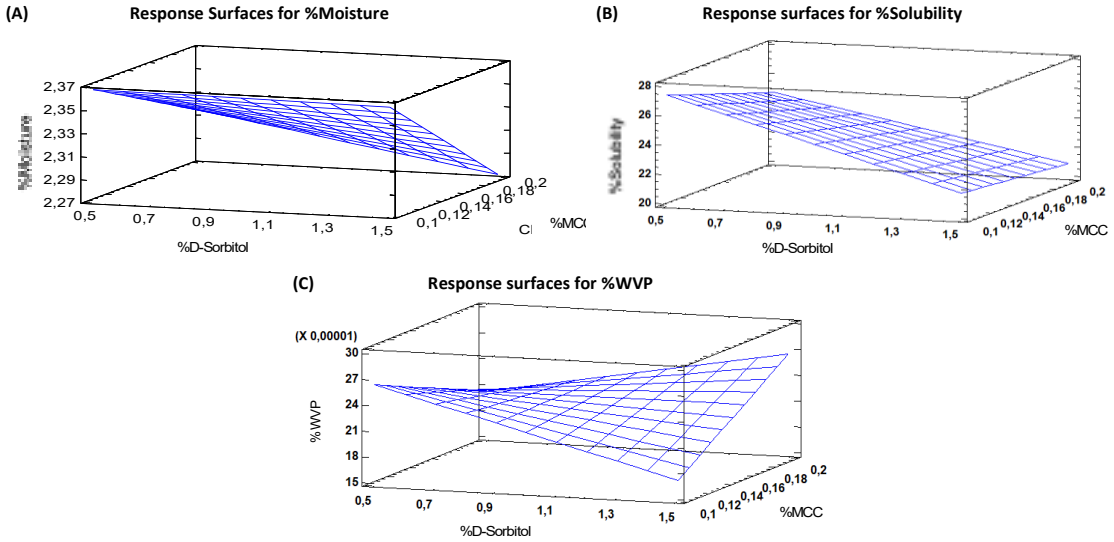

Figure 3. Response surfaces for %Moisture (A), %Solubility (B), and %WVP (C) of oxidized starch-based films by varying the %D-sorbitol and %MCC. Keys: WVP: Water vapor permeability; MCC: Microcrystalline cellulose.

CONCLUSION

The purpose of this research was to develop films using starch from Hass avocado seeds as a more environmentally friendly alternative to conventional plastics and fruit waste. To improve the mechanical and barrier properties of the films, a chemical modification of the neat starch was carried out at different reaction times, and varying percentages of D-Sorbitol as a plasticizer and MCC as a reinforcement were added.

The results showed that the oxidation time alters the starch structure, reflecting changes in hydroxyl groups and the addition of carbonyl and carboxyl functional groups, which significantly influence the properties of the oxidized starch, such as its swelling capacity, water absorption, and solubility.

To minimize moisture, solubility, and water vapor permeability in the films, the most suitable values were determined to be 1.5% D-Sorbitol and 0.1% MCC, which are the most appropriate for formulation in specific applications. Overall, these findings suggest that a more sustainable alternative can be provided for the production of films

and other products traditionally made with conventional plastic materials. It is important to note that the use of small percentages of MCC is essential to ensure adequate functionality in the films.

NOTES

AUTHOR CONTRIBUTIONS

Conceptualization and methodology, L. A. Cedeño-Sares; formal analysis, M. E. Yánez-Romero, D. Macas-Jiménez, M. Vidal-Zapata, H. L. Brito-Moína, and B. Lapo-Calderón; investigation, M. E. Yánez-Romero, D. Macas-Jiménez, and M. Vidal-Zapata; resources, H. L. Brito-Moína; writing – original draft preparation, M. E. Yánez-Romero; writing – review and editing, B. Lapo-Calderón and C. Beltrán-Balarezo; visualization, C. Beltrán-Balarezo; supervision, M. E. Yánez-Romero; project administration, L. A. Cedeño-Sares. All authors have read and agreed to the published version of the manuscript.

FUNDING

This work was supported by the Directorate of Research, Development and Innovation of the Technical University of Machala through institutional research funding.

INSTITUTIONAL REVIEW BOARD STATEMENT

Not applicable for studies not involving humans or animals.

INFORMED CONSENT STATEMENT

Not applicable because this study did not involve humans.

DATA AVAILABILITY STATEMENT

The data can be made available under request.

ACKNOWLEDGEMENTS

The authors would like to thank the Technical University of Machala for the institutional support provided for the execution of this research. They also appreciate the anonymous reviewers for their insightful comments and suggestions, which helped improve the quality of this manuscript.

CONFLICTS OF INTEREST

The authors declare no conflict of interest.

REFERENCES

ARAÚJO RG et al. 2020. Hydrothermal-microwave processing for starch extraction from Mexican avocado seeds: Operational conditions and characterization. Processes 8: 759.

AYO OMOGIE HN et al. 2022. Physicochemical, Functional, Pasting Properties and Fourier Transform Infrared Spectroscopy of Native and Modified Cardaba banana (Musa ABB) Starches. Food Chemistry Advances 1: 100076.

BALLESTEROS-MÁRTINEZ L et al. 2020. Effect of glycerol and sorbitol concentrations on mechanical, optical, and barrier properties of sweet potato starch film. NFS Journal 20: 1–9.

BARBOSA E et al. 2016. Chemical and technological properties of avocado (Persea americana Mill.) seed fibrous residues. Food and Bioproducts Processing 100: 457-463.

BARRAZA G & SICHE R. 2021. Almidón de semilla de palta: Optimización del índice de blancura durante el proceso de extracción. Agroindustrial Science 11: 81–85.

BUSTILLOS-RODRÍGUEZ JC et al. 2019. Physicochemical, Thermal and Rheological Properties of Native and Oxidized Starch from Corn Landraces and Hybrids. Food Biophysics 14: 182–192.

CALERO M et al. 2020. Estado del arte de bioplástico proveniente de los residuos agroindustriales del plátano (musa paradisiaca), para la producción de envases biodegradables. Revista Ingeniería e Innovación 9: 28–37.

CARHUALLAY O et al. 2020. Effect of sodium hypochlorite concentration and oxidation time on the degree of substitution of carboxyl groups, water absorption index and gelatinization temperature of Achira starch (Canna edulis Ker). Agroindustrial Science 10: 165–173.

CHAPUEL A & REYES J. 2019. Obtención de una película biodegradable a partir de los almidones de semilla de aguacate (Persea americana Mill) y banano (Musa acuminata AAA) para el recubrimiento de papaya. Universidad de Guayaquil 17T19:48:13Z.

CHATTOPADHYAY S et al. 1997. Optimisation of conditions of synthesis of oxidised starch from corn and amaranth for use in film-forming applications. Carbohydrate Polymers 34: 203–212.

CORREA V et al. 2019. Aprovechamiento de la semilla de aguacate (Persea americana Mill.) tipo Hass para la extracción de almidón. Aprovechamiento de La Semilla de Aguacate (Persea Americana Mill.) 83: 120–123.

DAO PH et al. 2017. Oxidized Maize Starch: Characterization and Effect of It on the Biodegradable Films.Ii. Infrared Spectroscopy, Solubility of Oxidized Starch and Starch Film Solubility. Vietnam Journal of Science and Technology 55: 395–402.

EL HALAL SLM et al. 2015. Films based on oxidized starch and cellulose from barley. Carbohydrate Polymers 133: 644–653.

FAOSTAT. 2024. FAOSTAT: Producción/Rendimiento de Aguacates en Ecuador 1994-2021. [https://www.fao.org/faostat/es/#data/QCL/visualize] Licencia: CC-BY-4.0 Consultado el 17 de septiembre de 2024.

FASUAN TO et al. 2018. Modification of amaranth (Amaranthus viridis) starch, identification of functional groups, and its potentials as fat replacer. Journal of Food Biochemistry 42: e12537

FAUST S et al. 2022. Effect of glycerol and sorbitol on the mechanical and barrier properties of films based on pea protein isolate produced by high-moisture extrusion processing. Polymer Engineering & Science 62: 95–102.

FONSECA LM et al. 2015. Oxidation of potato starch with different sodium hypochlorite concentrations and its effect on biodegradable films. LWT-Ciencia y Tecnología de Los Alimentos 60: 714–720.

FONSECA LM et al. 2018. Fabrication and Characterization of Native and Oxidized Potato Starch Biodegradable Films. Food Biophysics 13: 163–174.

GÓMEZ F & JIMÉNEZ A. 2022. Elaboración de películas biodegradables con policaprolactona y almidóncelulosa de la cáscara de plátano verde (Musa paradisíaca). Alimentos Ciencia e Ingeniería 28: 19–33.

HAZROL MD et al. 2021. Corn Starch (Zea mays) Biopolymer Plastic Reaction in Combination with Sorbitol and Glycerol 12: 242.

HIDAYATI S et al. 2015. The application of sorbitol in the production of biodegradable films from nata de cassava. Reaktor 15: 195.

JIMÉNEZ R et al. 2022a. Extraction of starch from Hass avocado seeds for the preparation of biofilms. Food Science and Technology 42: e56820.

JIMÉNEZ R et al. 2022b. Extraction of starch from Hass avocado seeds for the preparation of biofilms. Food Science and Technology 42: 1–6.

LANG H et al. 2022. Effect of Microcrystalline Cellulose on the Properties of PBAT/Thermoplastic Starch Biodegradable Film with Chain Extender. Polymers, 14: 4517.

MACENA JFF et al. 2020. Physico-chemical, morphological and technological properties of the avocado (Persea americana mill. cv. hass) seed starch. Ciencia e Agrotecnologia 44: 001420.

MARGARETTY E et al. 2019. The Effect of Reaction Time and pH on the Process of Sago Starch. Journal of Physics: Conference Series 1167: 1–8.

MARTINS SHF et al. 2022. Extraction and characterization of the starch present in the avocado seed (Persea americana mill) for future applications. Journal of Agriculture and Food Research 8: 100303.

MEDINA J et al. 2018. Hydrolytic degradation and biodegradation of binary mixes of polylactic acid (PLA) with plastic residues. Revista Ingeniería UC 25: 248–258.

MERCI A et al. 2019. Films based on cassava starch reinforced with soybean hulls or microcrystalline cellulose from soybean hulls. Food Packaging and Shelf Life 20: 100321.

MILLER K et al. 2021. Effects of glycerol and sorbitol on optical, mechanical, and gas barrier properties of potato peel-based films. Packaging Technology and Science, 34: 11–23.

MINISTERIO DEL AMBIENTE Y AGUA. 2020. Ecuador impulsa la gestión adecuada de residuos orgánicos en las ciudades – Ministerio del Ambiente, Agua y Transición Ecológica. Boletìn No 117.

MURILLO-MARTÍNEZ M et al. 2021. Propiedades fisicoquímicas y funcionales del almidón obtenido de dos variedades de batata (Ipomoea batatas). Biotecnología En El Sector Agropecuario y Agroindustrial 19: 117–127.

NORMA MEXICANA NMX-K-281-SCFI-2012. 2012. Concentración de Hipoclorito de Sodio en solución -método de prueba- (cancela a la NMX-K).

OSORIO PA & RUBIANO KD. 2019. Desarrollo de una biopelícula partiendo de cáscara de banano y fibra natural como agente de refuerzo a nivel laboratorio. Bogotá: Fundación Universidad de América.

OTHMAN SH et al. 2019. Tapioca starch films reinforced with microcrystalline cellulose for potential food packaging application. Food Science and Technology 39: 605–612.

PEDRESCHI R et al. 2022. Short vs. Long-Distance Avocado Supply Chains: Life Cycle Assessment Impact Associated to Transport and Effect of Fruit Origin and Supply Conditions Chain on Primary and Secondary Metabolites. Foods 11: 1807.

RIERA MA et al. 2018. Residuos agroindustriales generados en Ecuador para la elaboración de bioplásticos. Revista Ingeniería Industrial 17: 227–246.

RIERA MA & PALMA RR. 2018. Obtención de bioplásticos a partir de desechos agrícolas. Una revisión de las potencialidades en Ecuador. Avances En Química, 13: 69–78.

RINCÓN et al. 2007. Efecto de la acetilación y oxidación sobre algunas propiedades del almidón de semillas de Fruto de pan (Artocarpus altilis). Archivos Latinoamericanos de Nutricion, 57(3), 287–294.

RUILOBA I et al. 2018. Elaboración de bioplástico a partir de almidón de semillas de mango. Revista de Iniciación Científica 4: 28–32.

SÁNCHEZ H et al. 2021. Biofilms production from avocado waste. Ingenieria y Universidad 25: 16p.

SANTOS FKG dos et al. 2017. Effect of the Addition of Carnauba Wax on Physicochemical Properties of Chitosan Films. Materials Research 20: 479–484.

SCHAICH KM. 2016. Analysis of Lipid and Protein Oxidation in Fats, Oils, and Foods. In: HU M & JACOBSEN C. Oxidative Stability and Shelf Life of Foods Containing Oils and Fats. AOCS Press. p.1–131.

SOLARTE-MONTÚFAR JG et al. 2019. Propiedades Reológicas y Funcionales del Almidón. Procedente de Tres Variedades de Papa Criolla. Información Tecnológica 30: 35–44.

SUKHIJA S et al. 2017. Molecular characteristics of oxidized and cross-linked lotus (Nelumbo nucifera) rhizome starch. International Journal of Food Properties 20: S1065–S1081.

SURI S & SINGH A. 2023. Modification of starch by novel and traditional ways: influence on the structure and functional properties. Sustainable Food Technology 1: 348–362.

VANIER NL et al. 2012. Physicochemical, crystallinity, pasting and morphological properties of bean starch oxidised by different concentrations of sodium hypochlorite. Food Chemistry 131: 1255–1262.

VIVERO AS et al. 2019. Bioactive compounds and potential health benefits of avocado. Revista Chilena de Nutricion 46: 491–498.

WIJAYA C et al. 2019. Isolation and characterization of starch from Limnophila aromatica. Heliyon 5: e01622.

YADAV A et al. 2018. Biopolymers as packaging material in food and allied industry. International Journal of Chemical Studies 6: 2411–2418.

YAO DÉSIRÉ A et al. 2021. Starch-based edible films of improved cassava varieties Yavo and TMS reinforced with microcrystalline cellulose. Heliyon 7: e06804.

ZHOU F et al. 2016. Potato starch oxidation induced by sodium hypochlorite and its effect on functional properties and digestibility. International Journal of Biological Macromolecules 84: 410–417.